Available online at www.sciencedirect.com

ScienceDirect

journal homepage: www.jfda-online.com

Original Article

Pyrrolizidine alkaloid-derived DNA adducts are common toxicological biomarkers of pyrrolizidine alkaloid N-oxides

Xiaobo He [a], *Qingsu Xia* [a], *Kellie Woodling* [a], *Ge Lin* [b], *Peter P. Fu* [a,*]

[a] *National Center for Toxicological Research, U.S. Food and Drug Administration, Jefferson, AR 72079, United States*
[b] *School of Biomedical Sciences, Faculty of Medicine, The Chinese University of Hong Kong, Hong Kong*

ARTICLE INFO

Article history:
Available online 19 September 2017

Keywords:
Pyrrolizidine alkaloid
Pyrrolizidine alkaloid N-oxide
LC–ES–MS/MS
DHP–DNA adducts

ABSTRACT

There are 660 pyrrolizidine alkaloids (PAs) and PA N-oxides present in the plants, with approximately half being possible carcinogens. We previously reported that a set of four PA-derived DNA adducts is formed in the liver of rats administered a series of hepatocarcinogenic PAs and a PA N-oxide. Based on our findings, we hypothesized that this set of DNA adducts is a common biological biomarker of PA-induced liver tumor formation. In this study, we determined that rat liver microsomal metabolism of five hepatocarcinogenic PAs (lasiocarpine, retrorsine, riddelliine, monocrotaline, and heliotrine) and their corresponding PA N-oxides produced the same set of DNA adducts. Among these compounds, lasiocarpine N-oxide, retrorsine N-oxide, monocrotaline N-oxide, and heliotrine N-oxide are for first time shown to be able to produce these DNA adducts. These results further support the role of these DNA adducts as potential common biomarkers of PA-induced liver tumor initiation.

1. Introduction

Pyrrolizidine alkaloids (PAs) and PA N-oxides are toxic plant secondary metabolites present in numerous plant species [1–11]. PA-containing plants are the most common poisonous plants affecting livestock, wildlife, and humans, and a number of PAs are carcinogenic [1,6,7,12,13].

We recently determined that a set of four PA-derived DNA adducts was formed in the liver of female rats dosed with seven hepatocarcinogenic PAs and riddelliine N-oxide, but not formed from PAs that are not carcinogenic [14]. These four DNA adducts are a pair of epimers of 7-hydroxy-9-(deoxyguanosin-N^2-yl)dehydrosupinidine adducts (termed as DHP-dG-3 and DHP-dG-4) and a pair of epimers of 7-hydroxy-9-(deoxyadenosin-N^6-yl)dehydrosupinidine adducts (termed as DHP-dA-3 and DHP-dA-4) (Fig. 1). We have proposed that this set of DNA adducts (DHP-dG-3, DHP-dG-4, DHP-dA-3, and DHP-dA-4) is a common biological biomarker of PA-induced liver tumor formation [14,15]. We have also found that metabolism of PAs by rat liver microsomes generated four

* *Corresponding author*. Fax: +1 870 543 7136.
E-mail address: peter.fu@fda.hhs.gov (P.P. Fu).
http://dx.doi.org/10.1016/j.jfda.2017.09.001

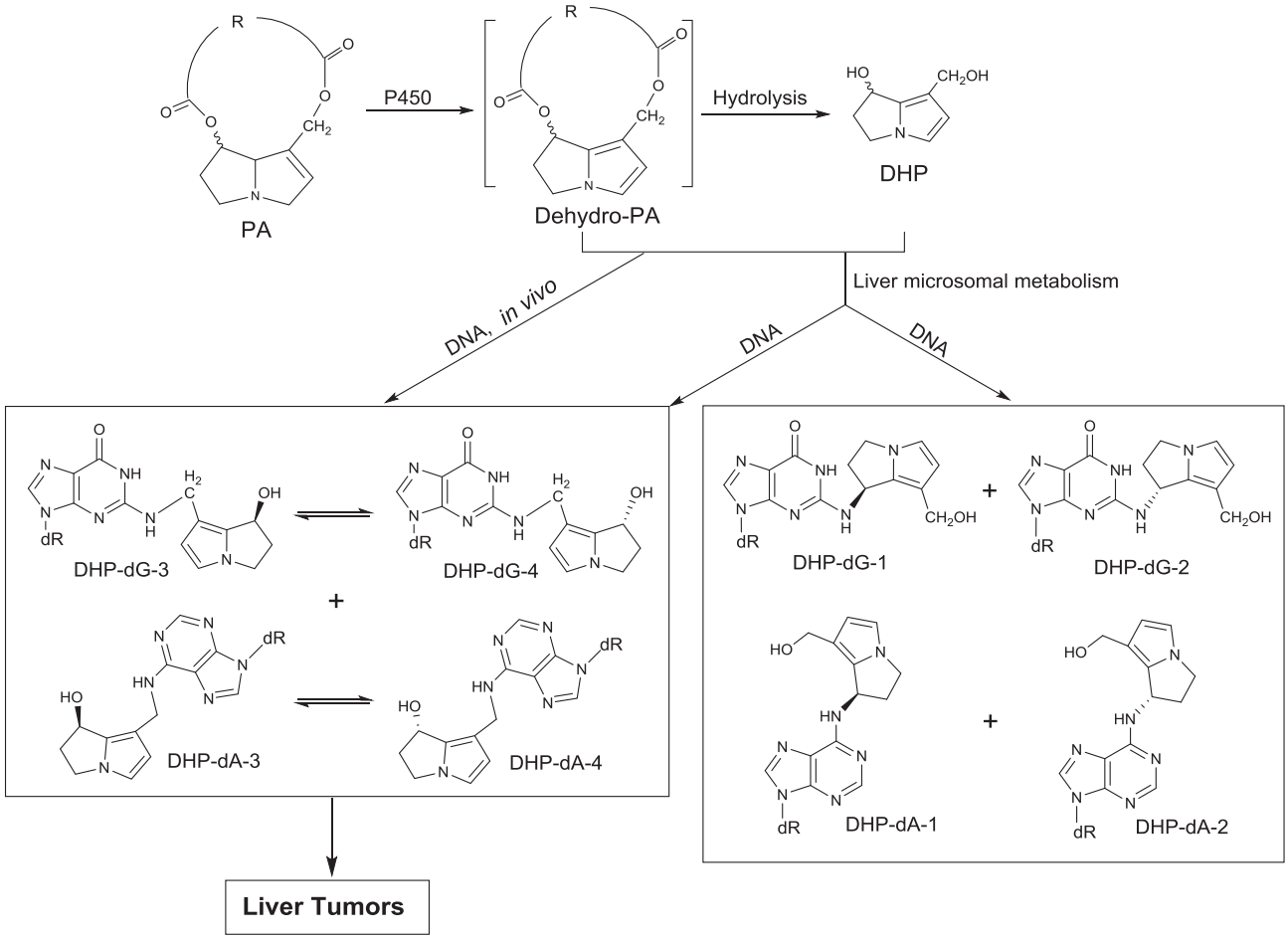

Fig. 1 – Formation of DHP–DNA adducts from the metabolism of PAs *in vivo* and *in vitro*. DHP designates 6,7-dihydro-7-hydroxy-1-hydroxymethyl-5*H*-pyrrolizine.

additional DHP–DNA adducts, designated as DHP-dG-1, DHP-dG-2, DHP-dA-1, and DHP-dA-2 (Fig. 1) [16].

There are 660 PAs and PA *N*-oxides present in the plants and approximately half are toxic and carcinogenic [1,6–11]. At present, only seven hepatocarcinogenic PAs (riddelliine, retrorsine, monocrotaline, heliotrine, clivorine, senkirkine, and lasiocarpine) and one PA *N*-oxide (riddelliine *N*-oxide) are known to produce these DHP–DNA adducts (DHP-dG-3, DHP-dG-4, DHP-dA-3, and DHP-dA-4) *in vivo* and/or *in vitro* [14,17,18]. It is important to study more PAs and/or PA *N*-oxides to determine whether or not this set of DHP–DNA adducts is a common biomarker of PA-induced liver tumor formation.

In the present study, we investigated the metabolism of five hepatocarcinogenic PAs (retrorsine, riddelliine, monocrotaline, lasiocarpine, and heliotrine) and their corresponding PA *N*-oxides (retrorsine *N*-oxide, riddelliine *N*-oxide, monocrotaline *N*-oxide, lasiocarpine *N*-oxide, and heliotrine *N*-oxide) by male F344 rat liver microsomes in the presence of calf thymus DNA. The structures of these PA *N*-oxides are shown in Fig. 2. We found that all these PAs and PA *N*-oxides produced the same DNA adducts. The non-carcinogenic PA, platyphylline, was also included for study.

2. Materials and methods

2.1. Chemicals

Monocrotaline, retrorsine, retrorsine *N*-oxide, calf thymus DNA (sodium salt, type I), nuclease P1, micrococcal nuclease (MN), spleen phosphodiesterase (SPD), and NADPH were purchased from Sigma–Aldrich (St. Louis, MO, USA). Heliotrine was purchased from Accurate Chemical & Scientific Corporation (Westbury, NY, USA). Lasiocarpine was purchased from PhytoLab (Dutendorfer, Germany). Dimethylformamide (DMF), acetonitrile, potassium carbonate, chloroform, diethyl ether, and phosphate buffered saline (PBS) were obtained from Fisher Scientific (Pittsburgh, PA, USA). All solvents used were LCMS or HPLC grade.

Riddelliine was obtained from Dr. Po-Chan, the National Toxicology Program (NTP). Platyphylline, which contains 70% platyphylline and 30% neoplatyphylline, was a gift from Prof. H.S. Chen at the Department of Phytochemistry, The Secondary Military Medical University, Shanghai, China. Riddelliine *N*-oxide, monocrotaline *N*-oxide, lasiocarpine *N*-oxide, and heliotrine *N*-oxide were synthesized by *N*-oxidation of the

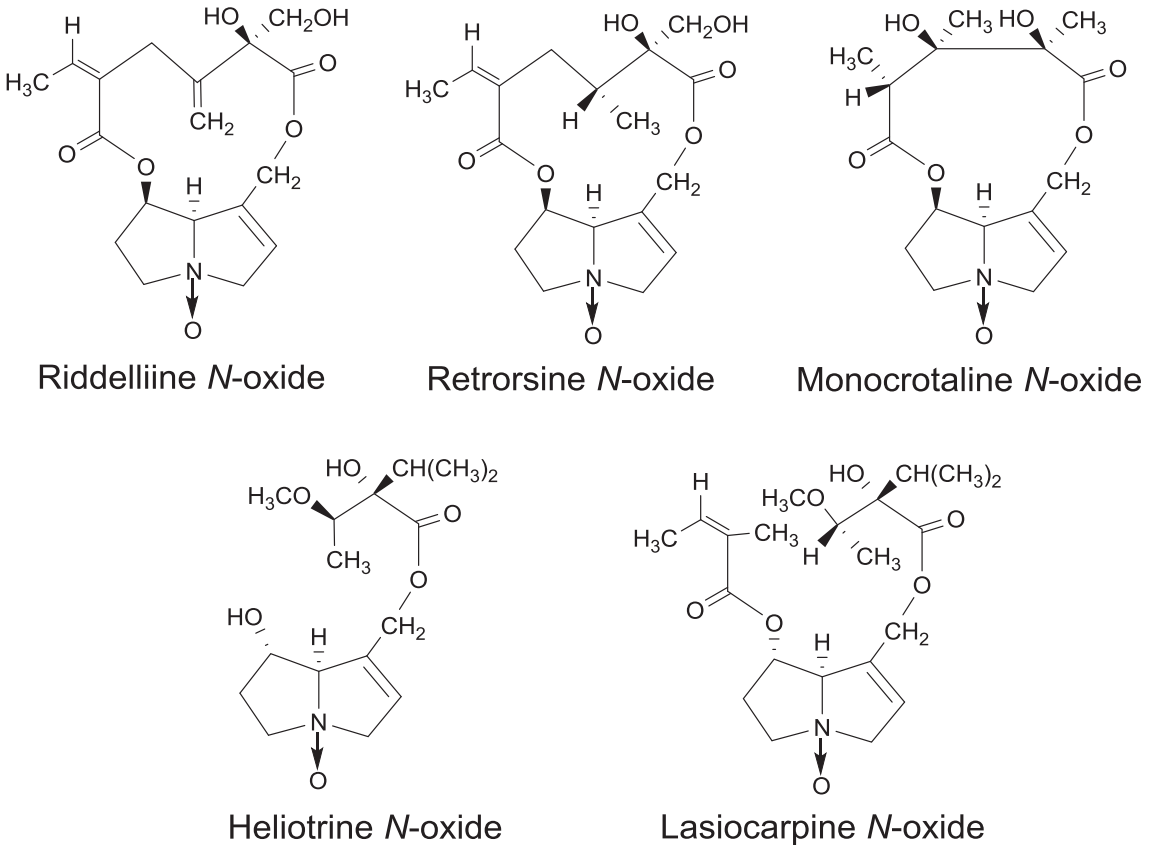

Fig. 2 – The structures of riddelliine N-oxide, retrorsine N-oxide, monocrotaline N-oxide, lasiocarpine N-oxide, and heliotrine N-oxide.

corresponding PAs with 30% hydrogen peroxide as previously described [19,20]. DHP-dG-1, DHP-dG-2, DHP-dG-3, DHP-dG-4, DHP-dA-1, DHP-dA-2, DHP-dA-3, and DHP-dA-4 adducts were synthesized as previously described [17,21]. Isotopically labeled DHP-[$^{15}N_5$]dG and DHP-[$^{15}N_5$ $^{13}C_{10}$]dA adducts, used as internal standards for quantitation of DHP-dG and DHP-dA adducts by LC/MS/MS, were synthesized as described previously [14,17,21].

2.2. Metabolism of PA N-oxides by male F344 rat liver microsomes in the presence of calf thymus DNA

The metabolism of PA N-oxides (riddelliine N-oxide, retrorsine N-oxide, monocrotaline N-oxide, lasiocarpine N-oxide, or heliotrine N-oxide) by F344 rat liver microsomes was conducted in a 1.0 mL incubation volume containing 100 mM sodium phosphate buffer (pH 7.6), 5 mM magnesium chloride, 1 mM NADPH, 1 mg/mL rat liver microsomes, 500 μM PA N-oxide, and 500 μg of calf thymus DNA at 37 °C for 60 min. After incubation, the reaction mixture was successively extracted with 1.0 mL of phenol, 1.0 mL of phenol/chloroform/isoamyl alcohol (v/v/v, 25/24/1), and 1.0 mL of chloroform/isoamyl alcohol (v/v, 24/1). The DNA in the aqueous phase was precipitated by adding 1/10 volume of 5 M sodium chloride followed by 2 volumes of cold ethanol and washed three times with 70% ethanol. The DNA samples were redissolved at 2 mg/mL in distilled water, and then enzymatically hydrolyzed to deoxynucleosides with micrococcal nuclease (MN), spleen phosphodiesterase (SPD), and nuclease P1 as previously described [14]. The resulting samples were spiked with internal standards for LC–ESI/MS/MS analysis. For comparison the metabolism of five corresponding PAs (riddelliine, retrorsine, monocrotaline, lasiocarpine, or heliotrine) by F344 rat liver microsomes was conducted.

2.3. Identification of metabolites formed from metabolism of riddelliine N-oxide by male F344 rat liver microsomes

The metabolism of riddelliine N-oxide by male F344 rat microsomes was conducted as described above with the exception that no calf thymus DNA was added. After incubation, the mixture was centrifuged at 105,000 g for 30 min at 4 °C to remove microsomal proteins. The supernatant was collected, and aliquots of 10 μL were directly subjected to LC/MS analysis.

2.4. LC–ESI/MS/MS analysis of DHP-dG and DHP-dA adducts formed in vitro

2.4.1. Liquid chromatography

A Finnigan Surveyor HPLC system was coupled with the TSQ mass spectrometer. The samples were loaded onto a reverse phase column (ACE 3 C18, 4.6 mm × 150 mm, 3 μm, MAC-MOD Analytical, Chadds Ford, PA) with mobile phases of methanol

and water (containing 2 mM ammonium acetate; pH 5.5) at a flow rate of 0.3 mL/min. The elution gradient began with 15% methanol for 5 min, followed by a linear gradient up to 65% methanol over the next 35 min, then methanol was increased to 95% in 1 min. After holding 95% methanol for 6 min, the gradient was reset to 15% methanol in 1 min. The column was equilibrated for 18 min before the next injection. The samples were maintained at 5 °C in the autosampler during the entire analysis.

2.4.2. *Mass spectrometry*

The same TSQ Quantum Ultra Triple Stage Quadrupole ES–MS/MS System was used for the DHP–DNA adduct analysis. The spray voltage was 3000 V, the vaporizer temperature was 400 °C, and the capillary temperature was 280 °C. The nitrogen pressure of sheath and auxiliary gases was 30 and 5 (arbitrary units), respectively. The argon collision gas pressure was 1.5 mTorr, the collision energy was 17 eV for DHP-dG and its internal standard; and 21 eV for DHP-dA and its internal standard.

A selected reaction monitoring (SRM) scheme was employed involving transitions of the $[M + H]^+$ precursor ions to selected product ions, with the following transitions: *m/z* 403 → *m/z* 269 for DHP-dG adducts; *m/z* 408 → *m/z* 274 for DHP-[$^{15}N_5$]dG internal standards; *m/z* 387 → *m/z* 253 for DHP-dA adducts; and *m/z* 402 → *m/z* 263 for DHP-[$^{15}N_5$,$^{13}C_{10}$]dA internal standards.

Data acquisition and reprocessing were performed using Thermo Xcalibur 2.0 SR2 software.

2.5. *Standard characterization and calibration curves*

Standard curves were generated by plotting the amount of standard compounds against the peak-area ratios of DHP-dG/dA standards to the corresponding labeled internal standards. Each sample was tested with a 10 μL injection volume containing 60 fmol DHP-[$^{15}N_5$]dG and 15 fmol DHP-[$^{15}N_5$,$^{13}C_{10}$]dA as internal standards. Since DHP-dG-3 and DHP-dG-4 adducts, as well as DHP-dA-3 and DHP-dA-4 adducts, are interconvertible [21], the levels of DHP-dG-3 and DHP-dG-4 were combined for quantitation; DHP-dA-3 and DHP-dA-4 levels were also combined.

2.6. *LC–ESI/MS/MS identification of metabolites from the metabolism of riddelliine* N*-oxide*

2.6.1. *Liquid chromatography*

A Finnigan Surveyor HPLC system was coupled with a TSQ mass spectrometer. The samples were loaded onto a Luna 3 μm C18 column (4.6 × 150 mm, Phenomenex) with the mobile phases consisting of (A) water (containing 0.01% formic acid, pH = 3.5) and (B) acetonitrile at the flow rate of 300 μL/min. A gradient elution was adopted as follows: 0–10 min, 3% B; 10–35 min, 3–20% B; 35–45 min, 20–50% B, 45–50 min, 50–90% B. The gradient will then be reset to 3% B and the column was equilibrated for 18 min before the next injection. The samples were maintained at 5 °C in the autosampler during the entire analysis.

2.6.2. *Mass spectrometry*

A TSQ Quantum Ultra Triple Stage Quadrupole MS/MS System (ThermoFinnigan, San Jose, CA, USA) was equipped with an atmospheric pressure ionization (API) electrospray (ESI) interface. The instrument was operated in positive ion mode. The spray voltage was set to 3500 V, the vaporizer temperature to 300 °C, and the capillary temperature to 300 °C. Nitrogen was used as sheath gas and auxiliary gas, and argon was the collision gas. Nitrogen pressures of the sheath and auxiliary gases were set to 30 and 5 (arbitrary units), respectively. Argon was the collision gas, and was set to 1.5 mTorr. A selected reaction monitoring (SRM) scheme was employed involving transitions of the $[M + H]^+$ (or $[M-H_2O + H]^+$) precursor ions to selected product ions, with the following values: *m/z* 154 → 106 for DHP; *m/z* 443 → 118 for 7-GS-DHP; *m/z* 239 → 152 for 7-cysteine -DHP; *m/z* 350 → 120 for riddelliine; and *m/z* 366 → 118 for riddelliine *N*-oxide.

3. Results

3.1. *Standard characterization and calibration curves*

HPLC–ES–MS/MS calibration curves were generated from the synthetically prepared DHP-dG-1, DHP-dG-1, DHP-dG-3, DHP-dG-4, DHP-dA-1, DHP-dA-2, DHP-dA-3, and DHP-dA-4 versus their respective DHP-[$^{15}N_5$]dG and DHP-[$^{15}N_5$ $^{13}C_{10}$]dA internal standards. The calibration curves were linear over the concentration range of 2–40 fmol for DHP-dG-1; 2–40 fmol for DHP-dG-2; 1–20 fmol for DHP-dA-1; 1–20 fmol for DHP-dA-2; 0.5–40 fmol for DHP-dG-3/4; and 0.4–50 fmol for DHP-dA-3/4. The best linear fit and least variability for the calibration curves were achieved with a weighting factor of 1/X, with the correlation coefficients (r^2) for all curves > 0.99.

3.2. *LC–MS/MS analysis of DHP-dG and DHP-dA adducts formed* in vitro

After the metabolism of each PA and PA *N*-oxide by rat liver microsomes in the presence of calf thymus DNA, DNA was isolated, enzymatically hydrolyzed, and the resulting DHP-dG and DHP-dA adducts were quantified by LC–MS/MS analysis with the SRM mode. Total samples included those from the vehicle control, five PA *N*-oxides, five of their corresponding PAs, and platyphylline.

Following our previously established LC–MS/MS conditions, DHP-dG-1 and DHP-dG-2 adducts were well separated from DHP-dG-3 and DHP-dG-4 adducts. Also, DHP-dA-1 and DHP-dA-2 adducts were separated from DHP-dA-3 and DHP-dA-4 adducts [14,21]. The overall results of the DHP-dG and DHP-dA adduct formation from each of treated PAs and PA *N*-oxides are summarized in Table 1.

Representative SRM chromatograms of the DHP-dG and DHP-dA adducts formed from the metabolism of retrorsine are shown in Fig. 3A. Fig. 3A-1 shows the isotope-labeled internal standards DHP-[$^{15}N_5$]dG-1, DHP-[$^{15}N_5$]dG-2, DHP-[$^{15}N_5$]dG-3, and DHP-[$^{15}N_5$]dG-4 adducts, each involving transition of the $[M+H]^+$ precursor ion *m/z* 408 to selected product ion *m/z* 274. Fig. 3A-3 depicts the labeled internal standards DHP-[$^{15}N_5$,$^{13}C_{10}$]dA-1, DHP-[$^{15}N_5$,$^{13}C_{10}$]dA-2, DHP-[$^{15}N_5$,$^{13}C_{10}$]dA-3, and DHP-[$^{15}N_5$,$^{13}C_{10}$]dA-4 adducts involving transition of *m/z* 402 to *m/z* 263. Fig. 3A-2 and A-4 presents the DHP-dG and DHP-dA adducts formed from the metabolism of retrorsine,

Table 1 – LC–MS/MS analysis of DHP-dG and DHP-dA adducts for metabolism of 50 μM PAs and PA N-oxides by rat liver microsomes in the presence of calf thymus DNA.

Chemicals	Levels of DHP-dG and DHP-dA/10^8 nucleotides[a]						
	DHP-dG-1	DHP-dG-2	DHP-dG-3/4	DHP-dA-1	DHP-dA-2	DHP-dA-3/4	Total DHP-dG and DHP-dA
Vehicle Control	<LOD	<LOD	<LOD	<LOD	<LOD	<LOD	<LOD
Lasiocarpine	4.94 ± 0.76	7.66 ± 1.49	6.44 ± 0.74	5.36 ± 1.25	2.23 ± 0.56	18.93 ± 1.87	45.55
Retrorsine	2.02 ± 0.27	2.80 ± 0.47	4.05 ± 0.64	1.60 ± 0.16	0.55 ± 0.08	12.79 ± 1.76	23.82
Riddelliine	1.69 ± 0.31	2.53 ± 0.37	3.48 ± 0.26	1.03 ± 0.23	0.55 ± 0.12	9.08 ± 1.14	18.36
Monocrotaline	1.44 ± 0.10	1.33 ± 0.20	1.52 ± 0.07	0.97 ± 0.30	0.46 ± 0.10	5.17 ± 0.97	10.88
Heliotrine	<LOD	<LOD	1.86 ± 0.16	<LOD	<LOD	6.85 ± 0.56	8.71
Lasiocarpine *N*-oxide	1.48 ± 0.22	1.31 ± 0.40	1.42 ± 0.44	0.64 ± 0.10	0.61 ± 0.13	6.48 ± 0.52	11.94
Retrorsine *N*-oxide	<LOD	<LOD	1.47 ± 0.16	0.44 ± 0.03	<LOD	6.19 ± 0.47	8.09
Riddelliine *N*-oxide	<LOD	<LOD	0.91 ± 0.06	0.37 ± 0.04	<LOD	1.53 ± 0.36	2.81
Monocrotaline *N*-oxide	<LOD	<LOD	0.74 ± 0.05	0.12 ± 0.20	<LOD	0.48 ± 0.12	1.34
Heliotrine *N*-oxide	<LOD	<LOD	0.85 ± 0.09	<LOD	<LOD	1.60 ± 0.16	2.44
Platyphilline	<LOD	<LOD	<LOD	<LOD	<LOD	<LOD	<LOD

LOD = limit of detection based upon the analysis of 45 μg DNA by HPLC–ES–MS/MS. Under experimental conditions, the LOD of DHP-dG-1/2 is 0.71, DHP-dG-3/4 is 0.71, DHP-dA-1/2 is 0.14, and DHP-dA-3/4 is 0.14 adducts per 10^8 nucleotides, separately.
[a] Aliquots of DNA (45 μg) were assayed by HPLC–ES–MS/MS. The data are presented as the mean ± SD, $n = 3$.

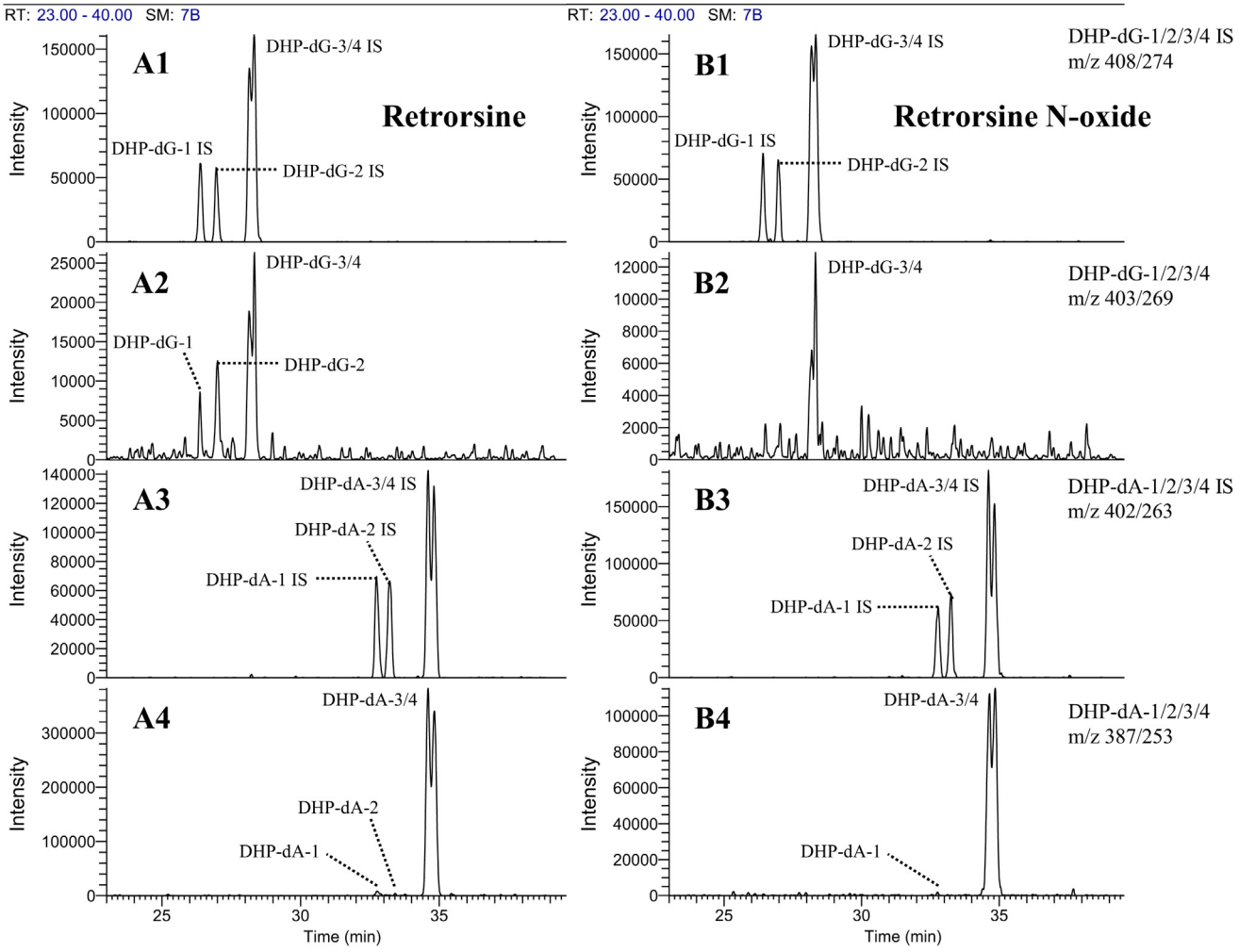

Fig. 3 – LC/MS SRM chromatograms of DHP-dG and DHP-dA adducts formed from the metabolism of (A) retrorsine and (B) retrosine *N*-oxide by rat liver microsomes in the presence of calf thymus DNA. IS: DHP-[$^{15}N_5$]dG and DHP-[$^{15}N_5$,$^{13}C_{10}$]dA labeled internal standards.

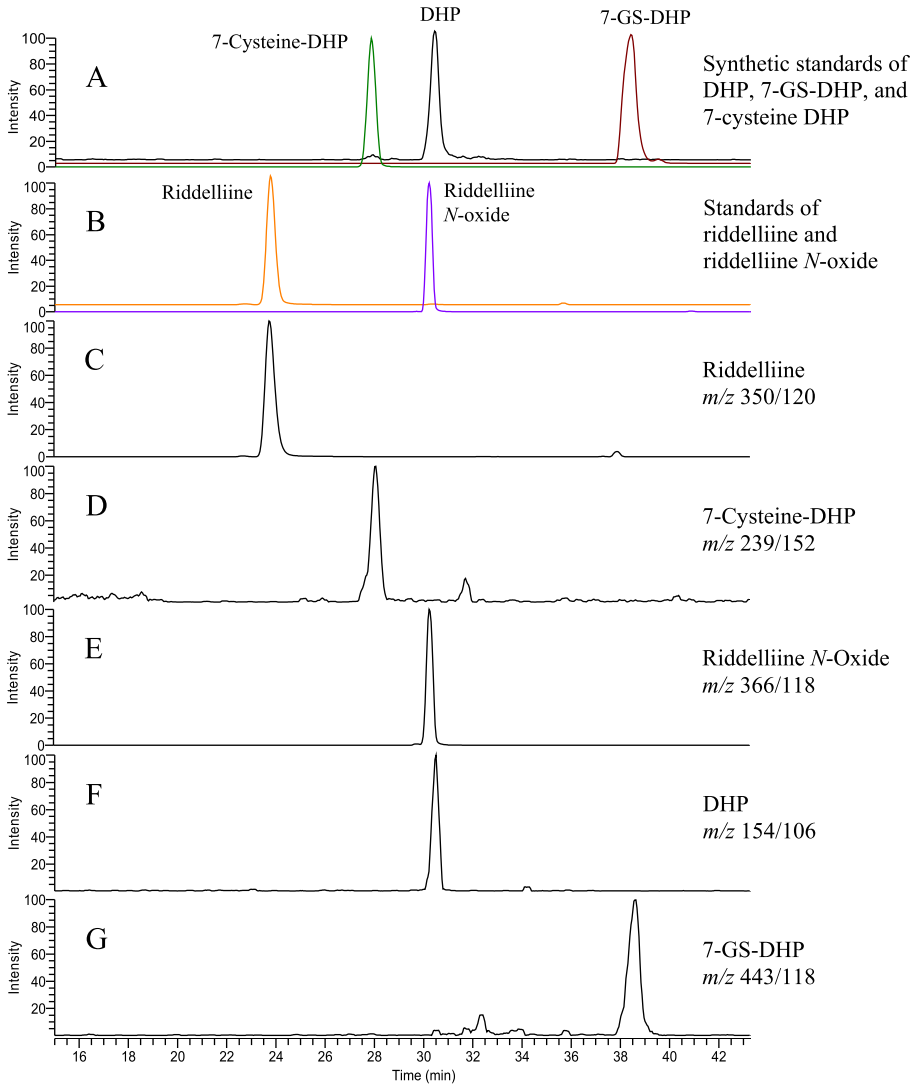

Fig. 4 – LC/MS SRM chromatograms of (A) and (B) synthetic standards of metabolites; and the metabolites of the rat liver microsomal metabolism of riddelliine N-oxide identified as (C) riddelliine; (D) 7-cysteine-DHP; (E) recovered substrate riddelliine N-oxide; (F) DHP; and (G) 7-GS-DHP.

with the results indicating that all four DHP-dG and four DHP-dA adducts were generated in different yields (Table 1).

The SRM chromatograms of retrorsine N-oxide are shown in Fig. 3B. The yields of the DHP–DNA adducts were lower than those from retrorsine, with DHP-dG-1, DHP-dG-2, and DHP-dA-2 being not detected (Table 1, Fig. 3B-2, B-4).

The results summarized in Table 1 indicate that the levels of DHP-dG and DHP-dA adducts are formed from PAs to a greater extent than from the corresponding PA N-oxides.

3.3. *LC–MS/MS analysis of metabolites formed from metabolism of riddelliine* N-*oxide* in vitro

The metabolism of riddelliine N-oxide by male rat liver microsomes was conducted and its metabolites were identified by comparison of their LC/MS/MS SRM mode profiles with those of the synthetic standards (Fig. 4). The LC/MS SRM chromatograms of the synthetic standards riddelliine, 7-cysteine-DHP, riddelliine N-oxide, DHP, and 7-GS-DHP are shown in Fig. 4 Panel A and Panel B. The identified metabolites include riddelliine (Panel C), 7-cysteine-DHP (Panel D), DHP (Panel F), and 7-GS-DHP (Panel G).

4. Discussion

We previously proposed that the set of DHP-dG-3, DHP-dG-4, DHP-dA-3, and DHP-dA-4 adducts is a biomarker responsible for PA-induced liver carcinogenicity [14–16,22]. To provide more experimental results to support the proposal, we investigated the metabolism of five hepatocarciogenic PAs and their corresponding PA N-oxides by male rat liver microsomes in the presence of calf thymus DNA. We found that all of these compounds formed the same set of DHP-dG and DHP-dA adducts (Table 1). Among these PAs, lasiocarpine N-oxide, retrorsine N-oxide, monocrotaline N-oxide, and heliotrine N-oxide have never been studied before. Thus, besides the 7 hepatocarcinogenic PAs

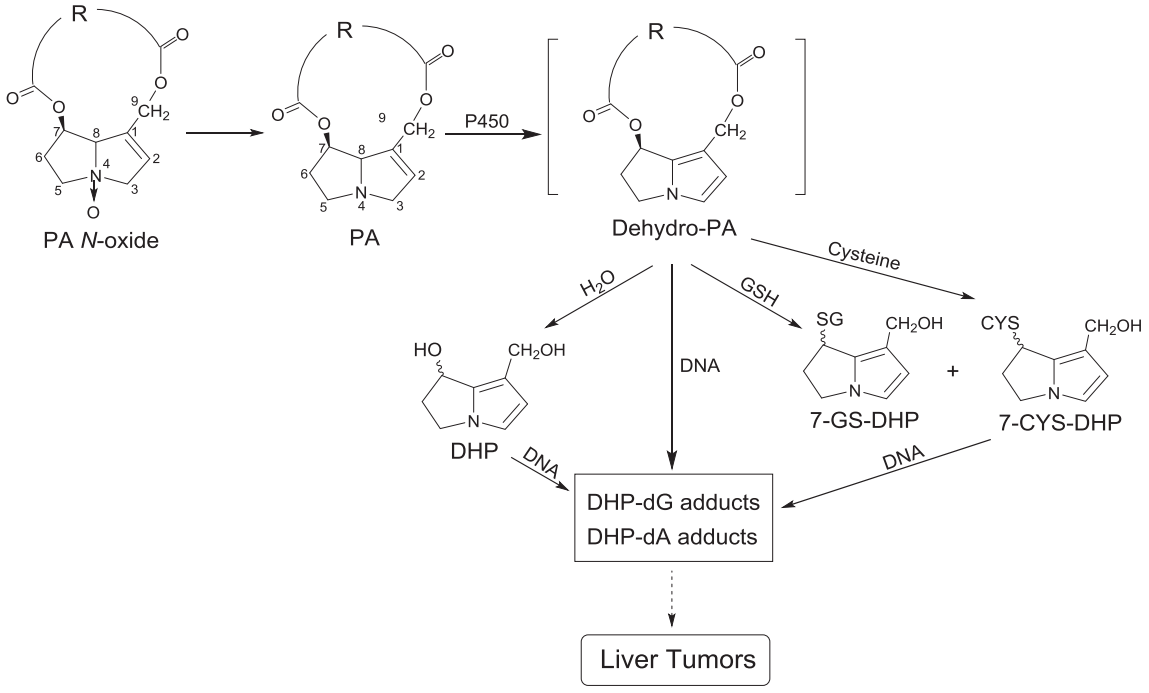

Fig. 5 – Proposed general metabolic activation pathways of PA N-oxides leading to the formation of pyrrolic DNA adducts and potential initiation of PA-induced liver tumors.

and riddelliine *N*-oxide that have previously been shown to produce these DHP–DNA adducts *in vivo*, these four PA *N*-oxides are a new addition to this category (formation of DHP–DNA adducts).

We previously studied the metabolism of riddelliine *N*-oxide by female F344 rat liver microsomes and only two metabolites, riddelliine and DHP, were identified [19]. In the present study by using LC/MS/MS analysis in SRM mode, we found that four metabolites, e.g. riddelliine, DHP, 7-glutathione-DHP (7-GS-DHP), and 7-cysteine-DHP, were formed from the metabolism of riddelliine *N*-oxide by male rat liver microsomes (Fig. 4). Both 7-GS-DHP and 7-cysteine-DHP have been found to be capable of binding with DNA to produce these DHP–DNA adducts *in vitro* and in HepG2 cells [16,18]. Based on our overall findings, we propose an expanded general metabolic activation pathway for toxic PA *N*-oxides leading to the formation of pyrrolic DNA adducts that potentially induce liver tumors (Fig. 5).

This proposed mechanism involves the formation of four reactive metabolites (dehydro-PA, DHP, 7-glutathione-DHP (7-GS-DHP), and 7-cysteine-DHP) that can bind with DNA to produce this set of DHP–DNA adducts. As such, there exist multiple activation pathways leading to the DHP–DNA adduct formation, and potentially PA *N*-oxide-induced, as well as PA-induced, liver tumor initiation.

To date, we have obtained the following findings that can support the role of this set of four DHP–DNA adducts as potential biomarkers of PA-induced (as well as PA *N*-oxide-induced) liver tumor formation:

1. Seven hepatocarcinogenic PAs and five PA *N*-oxide can produce a set of four DHP–DNA adducts *in vivo* and/or *in vitro* [14].
2. In conjunction with the NTP chronic tumorigenicity study, these DNA adducts were detected in the liver of female rats administered riddelliine [17].
3. Both male and female rat liver microsomes can biologically activate PAs and PA *N*-oxides to form these DHP–DNA adducts.
4. These adducts were also formed in the liver of male mice administered retrorsine [23].
5. The lifetime of the DHP–DNA adducts in the liver exhibited significant long persistence (up to 8 weeks) in mice *in vivo*, supporting their role in serving as biomarkers of PA exposure [23].
6. These four DHP–DNA adducts were also found in the livers of cows accidentally fed with PA-contaminated hay [24].

These overall experimental results well support our hypothesis that this set of DHP–DNA adducts can potentially be biomarkers of PA-induced liver tumor initiation. This also represents the first time that so many toxic xenobiotics are biologically activated through a common set of exogenous DNA adduct formation. Since humans are exposed to possibly 300 carcinogenic PAs and PA *N*-oxides present in our environment, for human health protection, further investigations of additional PAs and PA *N*-oxides are clearly warranted.

Acknowledgments

We thank Dr. Frederick Beland for his critical review of this manuscript. This research was supported in part by appointment (X. He) the Postgraduate Research Program at the NCTR administered by the Oak Ridge Institute for

Science and Education through an interagency agreement between the U.S. Department of Energy and the FDA. This article is not an official U.S. Food and Drug Administration (FDA) guidance or policy statement. No official support or endorsement by the U.S. FDA is intended or should be inferred. The authors declare no competing financial interest.

REFERENCES

[1] Edgar JA, Molyneux RJ, Colegate SM. Pyrrolizidine alkaloids: potential role in the etiology of cancers, pulmonary hypertension, congenital anomalies, and liver disease. Chem Res Toxicol 2015;28:4–20.
[2] Fu PP, Chiang HM, Xia Q, Chen T, Chen BH, Yin JJ, et al. Quality assurance and safety of herbal dietary supplements. J Environ Sci Health Part C, Environ Carcinog Ecotoxicol Rev 2009;27:91–119.
[3] Fu PP, Xia Q, Chou MW, Lin G. Detection, hepatotoxicity, and tumorigenicity of pyrrolizidine alkaloids in Chinese herbal plants and herbal dietary supplements. J Food Drug Anal 2007;15:400–15.
[4] Fu PP, Xia Q, Lin G, Chou MW. Pyrrolizidine alkaloids – genotoxicity, metabolism enzymes, metabolic activation, and mechanisms. Drug Metab Rev 2004;36:1–55.
[5] Huxtable RJ. Herbal teas and toxins: novel aspects of pyrrolizidine poisoning in the United States. Perspect Biol Med 1980;24:1–14.
[6] IPCS. Pyrrolizidine alkaloids. Environmental health criteria 80. International Programme on Chemical Safety. Geneva: WHO; 1988.
[7] Mattocks AR. Chemistry and toxicology of pyrrolizidine alkaloids. London, NY: Academic Press; 1986.
[8] Smith LW, Culvenor CCJ. Plant sources of hepatotoxic pyrrolizidine alkaloids. J Nat Prod 1981;44:129–52.
[9] Wiedenfeld H, Edgar J. Toxicity of pyrrolizidine alkaloids to humans and ruminants. Phytochem Rev 2011;10:137–51.
[10] Roeder E. Medicinal plants in China containing pyrrolizidine alkaloids. Pharmazie 2000;55:711–26.
[11] Roeder E. Medicinal plants in Europe containing pyrrolizidine alkaloids. Pharmazie 1995;50:83–98.
[12] Prakash AS, Pereira TN, Reilly PE, Seawright AA. Pyrrolizidine alkaloids in human diet. Mutat Res 1999;443:53–67.
[13] Stegelmeier BL, Edgar JA, Colegate SM, Gardner DR, Schoch TK, Coulombe RA, et al. Pyrrolizidine alkaloid plants, metabolism and toxicity. J Nat Toxins 1999;8:95–116.
[14] Xia Q, Zhao Y, Von Tungeln LS, Doerge DR, Lin G, Cai L, et al. Pyrrolizidine alkaloid-derived DNA adducts as a common biological biomarker of pyrrolizidine alkaloid-induced tumorigenicity. Chem Res Toxicol 2013;26:1384–96.
[15] Fu PP. Pyrrolizidine alkaloids: metabolic activation pathways leading to liver tumor initiation. Chem Res Toxicol 2017;30:81–93.
[16] Xia Q, Ma L, He X, Cai L, Fu PP. 7-Glutathione pyrrole adduct: a potential DNA reactive metabolite of pyrrolizidine alkaloids. Chem Res Toxicol 2015;28:615–20.
[17] Fu PP, Chou MW, Churchwell M, Wang Y, Zhao Y, Xia Q, et al. High-performance liquid chromatography electrospray ionization tandem mass spectrometry for the detection and quantitation of pyrrolizidine alkaloid-derived DNA adducts *in vitro* and *in vivo*. Chem Res Toxicol 2010;23:637–52.
[18] He X, Xia Q, Fu PP. 7-Glutathione-pyrrole and 7-cysteine-pyrrole are potential carcinogenic metabolites of pyrrolizidine alkaloids. J Environ Sci Health, Part C 2017;35:69–83.
[19] Chou MW, Wang YP, Yan J, Yang Y-C, Beger RD, Williams LD, et al. Riddelliine *N*-oxide is a phytochemical and mammalian metabolite with genotoxic activity that is comparable to the parent pyrrolizidine alkaloid riddelliine. Toxicol Lett 2003;145:239–47.
[20] Ruan J, Li N, Xia Q, Fu PP, Peng S, Ye Y, et al. Characteristic ion clusters as determinants for the identification of pyrrolizidine alkaloid *N*-oxides in pyrrolizidine alkaloid-containing natural products using HPLC–MS analysis. J Mass Spectrom 2012;47:331–7.
[21] Zhao Y, Xia Q, Gamboa da Costa G, Yu H, Cai L, Fu PP. Full structure assignments of pyrrolizidine alkaloid DNA adducts and mechanism of tumor initiation. Chem Res Toxicol 2012;25:1985–96.
[22] He X, Xia Q, Ma L, Fu PP. 7-Cysteinyl-pyrrole conjugate – a new potential DNA reactive metabolite of pyrrolizidine alkaloids. J Environ Sci Health, Part C 2016;34:57–76.
[23] Zhu L, Xue J, Xia Q, Fu PP, Lin G. The long persistence of pyrrolizidine alkaloid-derived DNA adducts in vivo: kinetic study following single and multiple exposures in male ICR mice. Arch Toxicol 2017;91:949–65.
[24] Fu PP, Xia Q, He X, Barel S, Edery N, Beland FA, et al. Detection of pyrrolizidine alkaloid DNA adducts in livers of cattle poisoned with *Heliotropium europaeum*. Chem Res Toxicol 2017;30:851–8.